Fluid Structure Interaction with RBF Morph A Generic Formula 1 Front End

Dr. Marco Evangelos Biancolini

University of Rome "Tor Vergata" – Department of Industrial Engineering

Rome, Italy

Email: biancolini@ing.uniroma2.it

Web: www.rbf-morph.com

Summary

A method for fluid structure interaction numerical modelling is herein presented. The volume mesh used for CFD calculations is parameterized according to FEM computed structural modal shapes thanks to a morpher. Modal loads are directly integrated over the CFD mesh and allow to calculate actual values of modal coordinates both for static and transient problems. Such parametric CFD model with modes embedded becomes flexible, i.e. capable to deform its shape under structural loads without the need to further interact with structural FEM model. Proposed method is demonstrated with an industrial application, the steady study of a flexible Formula 1 front wing, using the following commercial software: **NX Nastran** and **ANSYS Fluent**® coupled with the mesh morphing add-on **RBF Morph**™.

Keywords

Fluent, RBF Morph, modal analysis, FSI (Fluid Structure Interaction)

Background

Fluid structure interaction phenomena introduce an high level of complexity in the analysis methods; however there are applications that cannot be faced neglecting such interaction. The interaction can be the working principle of the component itself (reed valves action, parachute canopy unfolding, movement of a sheet of paper within a printing device, …); can be due to the lightweight design of the structure (aircraft design); or can be exploited to finely tune the design taking advantage of interaction (Formula 1 wings).

Our research group focus on FSI was driven in the past for the solution of an industrial problem: the reed valve movement [1] used for metering a secondary air flow within the exhaust system of a two strokes engine [2]. A custom FEM solver for planar beam (both FORTRAN and C implementations) has been developed and coupled to the gasdynamic solver developed at the University of Perugia and to the commercial solver **BOOST** by **AVL**. The approach has been extended integrating the same solver within **Fluent** (2D solutions) getting very interesting results for reed valves internal flow simulation [3]. The approach has been further extended to industrial applications: movement of a sheet of paper driven by jet flows within a printing device (2D and 3D with explicit FEM) [4], Formula 1 front wing analysis [5] (in this case mass and stiffness matrixes were precomputed using FEM solver **Nastran**), 3D analysis (see Figure 1) of a complete inlet system for two strokes engines controlled by six petals [7]. The most important achievement for 3D were collected and published in 2008 [6].

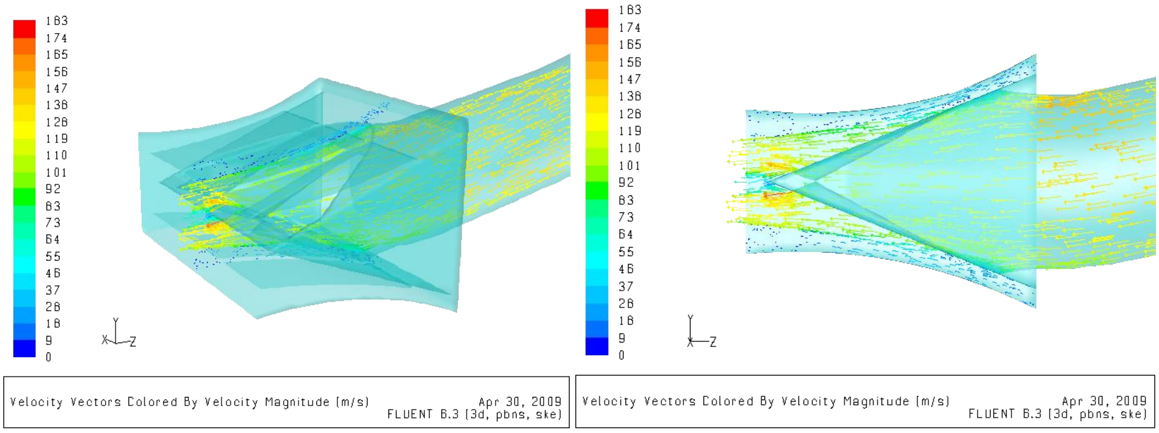

Figure 1:Coupled FSI analysis of a reed valve pack for two strokes engines [7]. Each petal movement is resolved tank to a custom structural dynamic solver embedded within Fluent using UDF.

All aforementioned examples have been faced using FSI weak coupling. All bottlenecks related to data exchanging were avoided thanks to the embedding of structural dynamic solver directly within the CFD solver **Fluent**, it's important to notice that usually the computational load required by the structural part is about 1-2% of the total. The weakness of such approach are: the implementation is quite complex and solver dependent, conformal meshes are used at the interface and the tuning of moving mesh algorithms used by **Fluent**. The smoothing of the volume mesh is one of the most important issue for FSI: a very good morpher is required to properly accommodate the structural deflections of the structure in the volume mesh; **Fluent** comes with a spring model for smoothing that is very fast but can easily produce reversed cells, results can be improved if the CFD mesh is deformed using an elastic solution [8]; the quality is good but the method is mesh dependent and difficult to extend to generic elements and parallel calculation. A better approach is given by the Radial Basis Functions (RBF) that combines the precision of mesh methods with the advantages of a meshless approach (parallelism, managing of generic elements). An interesting example about insect flight simulation using **OpenFOAM** and RBF for moving mesh is given in [9], in reference [10] the high quality of RBF is demonstrated showing that it can be very useful not only for FSI but for shape parameterization as well [11]. However quoted studies are limited to small academic application using approach that are not still mature for the industrial size of current CFD models.

The first industrial implementation of RBF for *mesh morphing* of large CFD models is **RBF Morph** [12], developed first as an on-demand module for a Formula 1 top team and then placed on the market as an add-on for the CFD solver **ANSYS Fluent** [13, 14]. A comprehensive description of the theory of the tools and its applications is given in [15].

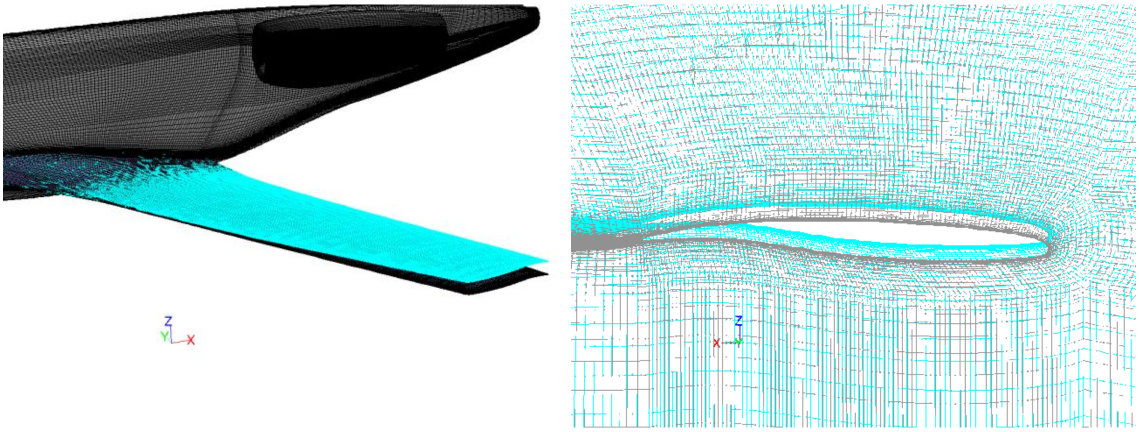

Figure 2: Aeroelastic analysis of an aircraft [16].FEM displacement field under flight loads is used to update the CFD mesh until convergence.

RBF Morph has proven to be effective also for FSI industrial problems; the first example has been conducted during a partnership with **Piaggio Aero** [16] with the aim to account for elastic deformation during a CFD steady analysis; a poor agreement between experiments and simulation was observed because of the large deflection of the wing (CFD simulation using the commercial solver **CFD++** using about 14 millions of hexahedra, see Figure 2), especially at wing tip. Using [17] as a reference the simulation workflow has been enhanced using mesh morphing (**Fluent** and **RBF Morph** for mesh updating, **Nastran** for the evaluation of deformed shape and **Patran** to map CFD loads on the structure) improving substantially the correlation between simulations and experiments.

The same approach has been successfully used for Formula 1 wings. Although effective, the chain is quite complex because each FSI iteration requires data exchanging. A new method, based on modal theory, has been defined to reduce the quantity of information exchanged between CFD and FEM solvers and is herein presented.

Proposed Approach

A modal basis of the structure is first extracted using a generic FEM solver (**NX Nastran** in this example), using mass normalization so that only modal frequencies need to be exchanged. Modal shapes of wing and pylons are then exported as a points cloud with known displacements (each FEM node is exported as an RBF point) and used as input data for the mesh morphing tool **RBF Morph**.

The generic point format used in **RBF Morph** can be used to import modes coming from a generic FEM solver; a specific implementation for **Nastran** output format is available as well. The output is extracted from the ASCII file "*.pch" generated using the standard option PUNCH of **Nastran**; mesh is directly imported from the standard "*.bdf" file parsing the relevant input CARDS (Nastran Data Deck). As explained in the first section, **RBF Morph** is an add-on module for the CFD solver **ANSYS Fluent**, and allows to enhance it providing to the user new functions for advanced mesh movement.

The set-up of **RBF Morph** is straightforward and typically consists of a set of surfaces controlled by the FEM extracted points (no matter if meshes are not conformal even if the FEM one is coarser, the high quality of RBF interpolation gently interpolate the elastic field everywhere on the CFD surface), a second set of surfaces that have to be preserved in the original position and a box to limit the morpher action only in the volume affected by structural deformation.

The procedure is then automatically extended to all the modes; so they will be available as standard **RBF Morph** shapes and can be superimposed using the multi parameter feature of the morpher (i.e. the user can assign a set of modal coordinates and update the complete mesh accordingly). To activate the advanced FSI functions the **(rbf-fmorph)** module has to be initialized, this operation will store in memory all the info required to update the shape of the volume mesh during the calculation (steady or transient). The module allows to calculate the modal surface integral directly within the CFD mesh; for the steady case the modal coordinates are calculated simply dividing the modal force by the squared circular frequency (i.e. the modal stiffness). The transient case (not considered in this paper) can be managed as well integrating the time history of modal coordinates.

A reference solution obtained by a complete two ways FSI approach is generated to evaluate modal approach convergence. The FSI mapping module of **Fluent** is used in this case to export pressure data to the FEM model, the mesh updating is similar to the one already described for modes, but in this case the static solution is used to update the CFD model shape.

It is worthwhile to notice that structural modes embedding method allows to perform FSI simulation without the need of exchanging information between FEM and CFD. Once the modes are transferred the CFD model becomes elastic, i.e. capable to update its shape under actual loads, even if boundary conditions are changed.

Test Case Description

The front end of a Formula 1 car is investigated. The geometry is represented in Figure 3; it includes the body, the front wheel, the pylon and the front wing composed by Main and Flap connected to the end plate, a fence limits the transversal flow.

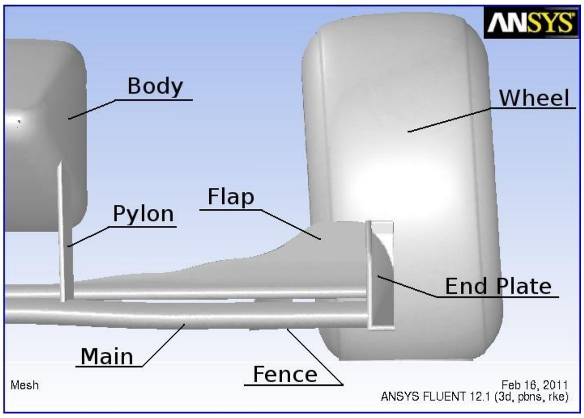

Figure 3: Geometry of the Formula 1 Front End.

The main is connected to the body by the pylons, the flap is connected to the main at the end plate making the assembly quite flexible so that important deformations are expected. The geometric model is property of ANSYS Inc.; a CAD model and several **Fluent** meshes (tetrahedral, hexcore, polyhedral) are available. For this FSI study the tetrahedral mesh has been considered. It is composed by about 3 millions of cells, the boundary layer is resolved thanks to 3 layers of prisms at the walls. The FEM mesh is the same surface mesh of the CFD model built with shell elements; an equivalent material thickness has been tuned to have a maximum displacement of 7 mm at 126 km/h.

Solution Workflow

Mode embedding is conducted using TUI and GUI commands of **RBF Morph**. The FEM field is prescribed to a first surface set that includes the deformable parts (the wing and the pylon), a second surface set is used to constrain the wheel, the body and the ground. The morpher action is limited using a box using a point distribution fine enough to guarantee a zero field at box boundary. Set-up is summarized in figure 4; surface points are highlighted on the left (green for points controlled using FEM solution, red for points constrained); all the RBF points are represented on the right. This manual set-up is conducted only for the first mode and refined until a good results is reached using the preview tools available both for surface and for volume mesh. The same set-up is then automatically replicated for all the modes using a simple script.

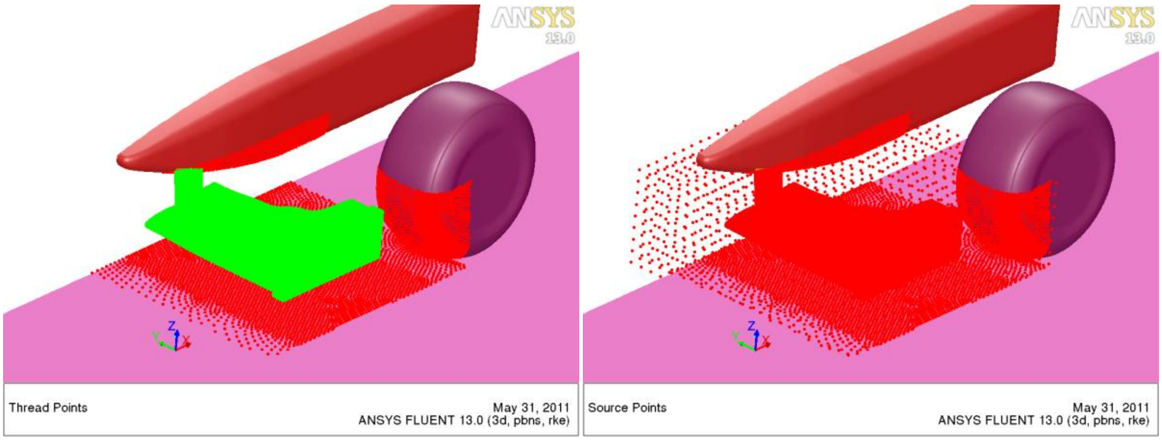

Figure 4: Set-up of RBF Morph.

The set-up is then completed using the **(rbf-fmorph-init)** that allows to load all the solution (modes) in the memory so that each subsequent mesh deformation for a given set of modall coordinates will be very fast, furthermore the initialization enables the surface integral command **(rbf-fmorph-forces)**. The FSI module is terminated using the **(rbf-fmorph-end)** command.

Mesh update is automated by a standard *calculation activity* of **Fluent** that calls the scheme command **(modal-q-update-static)** each 25 iterations. The command syntax is:

```
(define (modal-q-update-static)
;; calculate modal forces
(set! modal-forces (rbf-fmorph-forces '("front_wing_flap" ... "fin")))
;; update q = F / k
(set! modal-q (map / modal-forces modal-k))
;; update mesh
(rbf-fmorph (list (list "mode1-new" (list-ref modal-q 0)) ...)))
)
```

The **(modal-forces)** function retrieves a list of modal forces (a scalar for each mode) on the surface list used as argument. The **(modal-q)** variables are computed dividing the modal forces by the modal stiffness (i.e. the squared circular frequency). The mesh is then updated using the current values of modal coordinates with the **(rbf-fmorph)** command.

Results

Embedded modes are first verified using the preview tool that allows to show the effect of a generic shape modifier (or a superposition of several ones) on a portion of the CFD model; a combination of the first four modes is represented in figure 5 where the effect of each mode is highlighted using an amplification equal to 0.02; actual values depends of course on the surface loads.

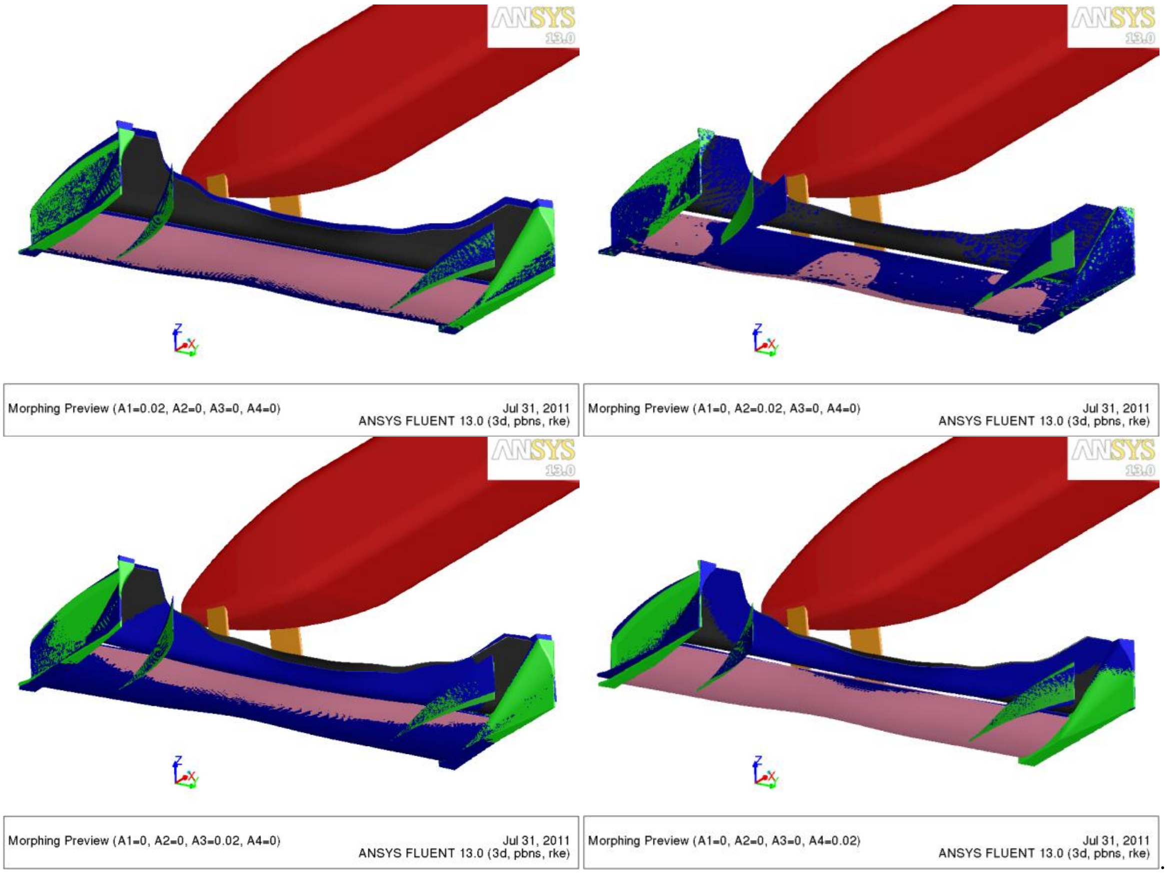

Figure 5: First 4 modes as embedded in the CFD model, highlighted using the preview tool. The first one is global of the whole wing (vertical displacement and rotation), the second is a local deflection of the fence, the third is a movement of the flap, the fourth is a global movement of the overall wing (with nodal lines at pylons and maximum displacement at the end plates).

Full coupled solution is a good reference for the evaluation of the convergence of modal method with respect to mode introduced; the preview tool is not only limited to a graphical representation, maximum displacement and surface mesh skewness are reported as well. Six solution are used in this case, the first five modes and the full coupled solution so that the modal solution and the full solution can be easily combined.

Mode	**Max d [mm]**	**Max err [mm]**	**Max err [%]**
1	5,58	1,61	22,39
2	6,33	0,86	12,00
3	6,34	0,85	12,15
4	6,53	0,66	9,50
5	7,00	0,19	2,76
2 Ways FSI	7,19	0,00	0,00

Table 1:Maximum displacement at 126 km/hr; comparison between full coupled method and modal method increasing the number of included modes.

If the modes are amplified using modal coordinates values at convergence and the full solution is subtracted applying a -1 amplification the error field is directly obtained as the deformation of the mesh; the contribution of high order modes can be deleted making zero their weight. The results are summarized in table 1; the higher error is predicted using only the first mode (22.4%) the error becomes lower than 3% (2.76%) if five modes are introduced. This is a known property of the modal base and it is interesting to notice that the error shape using ***i*** modes has typically the shape of the ***i* + *1*** mode.

In order to understand the role of compliance at the reference speed a comparison between forces calculated on the rigid model and the forces evaluated on the flexible one has been conducted. Results are summarized in table 2 where the loads obtained using the flexible model and the difference with respect to the rigid case are reported. The effect on drag is very high (about 10 %) and the downforce is affected as well (1.5%).

Part	**Fx [N]**	**Fy [N]**	**Fz [N]**	**dFx [%]**	**dFy [%]**	**dFz [%]**
Fin	1,00	1,21	0,07	-0,52	2,93	1,21
Flap	30,56	-0,38	-67,30	3,84	-23,15	0,35
Main	12,61	6,48	-319,94	30,60	-2,22	1,73
Plate	5,45	11,48	-19,37	5,12	-1,18	1,07
Vane	4,95	19,23	-0,71	3,41	1,70	-1,50
Total	54,57	38,02	-407,25	10,04	0,45	1,46

Table 2: Aerodynamic forces (Fx is the drag, Fz is the lift, Fy is the transversal load acting on the half model) calculated using the deformable model, the difference (dFx, dFy, dFz) are with respect to the rigid model.

The example has been completed investigating the effect of speed on drag and downforce in the range 54 km/hr – 162 km/hr; it is important to notice that enabling the mesh updating each 25 iteration the convergence is achieved in about 250 iterations, at the same cost of a standard simulation with rigid walls; furthermore the complete parametric analysis has been conducted during the same **Fluent** session without the need to reload modes (an hybrid initialization of the flow is used each time that the speed is updated). Obtained results are used to generate pressure maps and pathlines represented in figures 6 and 7.

The performance of proposed approach are summarized in table 3: the CPU time required for mesh updating is very low if compared with the cost of a single CFD iteration; so even a a transient analysis can be faced with a computational cost similar to the rigid case avoiding the high computational load required for data exchanging at each time step required for a full coupled two ways transient analysis.

Task	**Time [s]**	**Time [days]**
CPU Time to fit each mode (120.000 RBF points)	190	-
CPU Time to init 5 modes	117	-
CPU Time for each mesh update using 5 modes	3	-
CPU Time for a CFD iteration	15	-
User Time to set-up modes	-	0,5
User Time to set-up CFD + modal simulation	-	0,5

Table 3: Performances of proposed approach using a laptop Linux 64 bit, Intel® Centrino2 dual-core processor, 2.26GHz 8GB, RBF Morph 1.3 e Fluent 13.

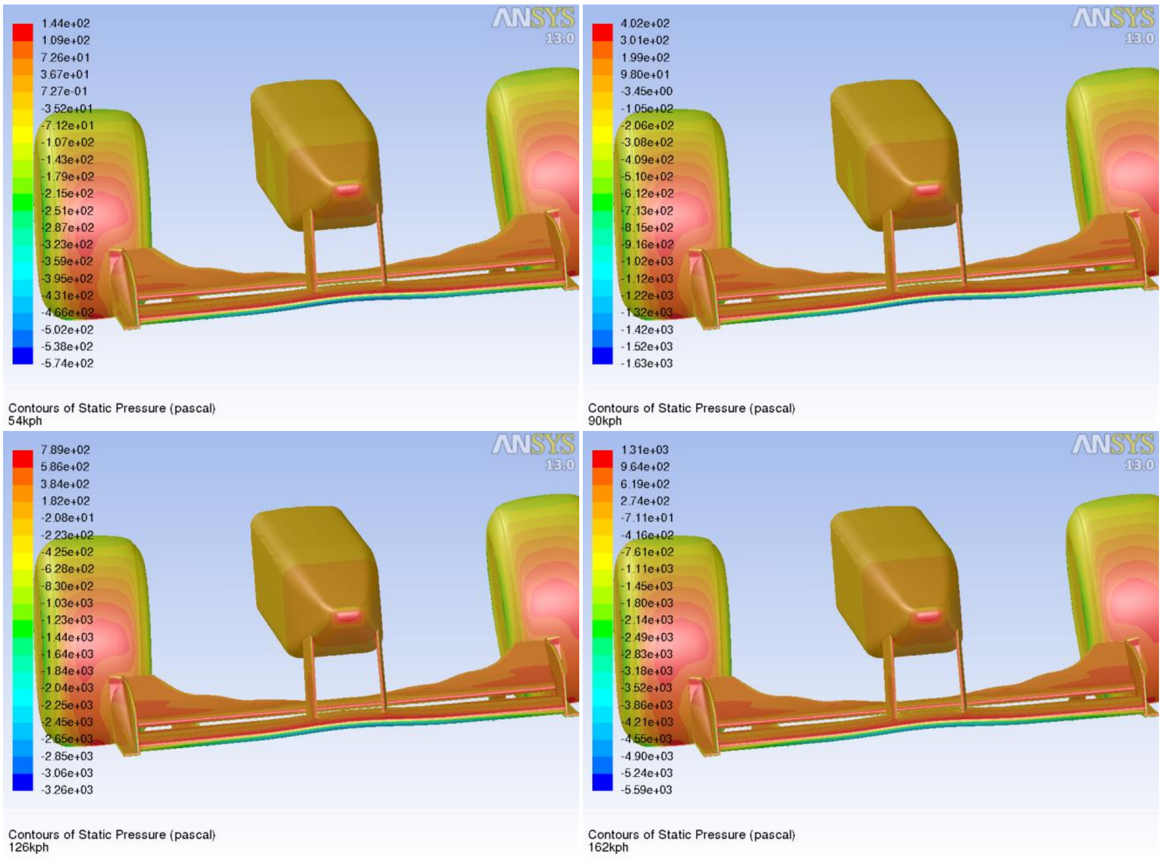

Contours of Static Pressure (pascal)
54kph

Contours of Static Pressure (pascal)
90kph

Contours of Static Pressure (pascal)
126kph

Contours of Static Pressure (pascal)
162kph

Figure 6: Pressure map for different values of car speed.

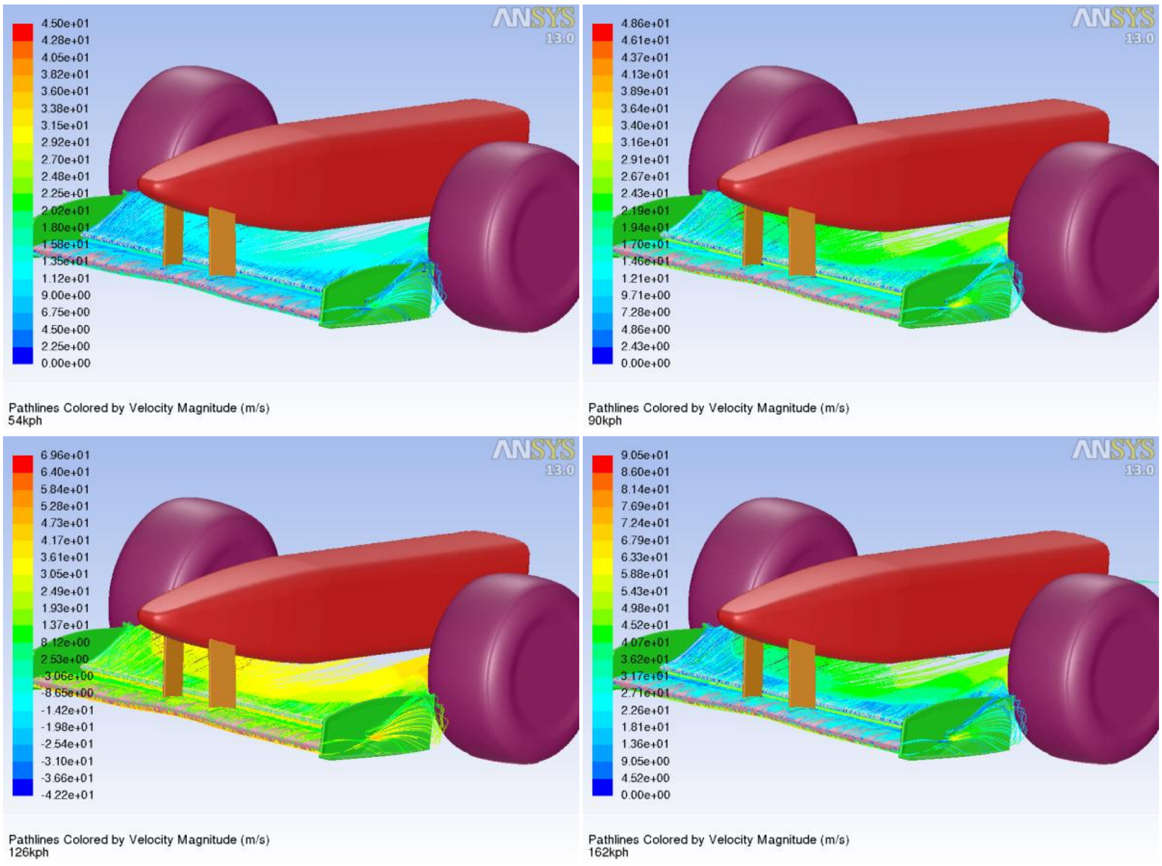

Pathlines Colored by Velocity Magnitude (m/s)
54kph

Pathlines Colored by Velocity Magnitude (m/s)
90kph

Pathlines Colored by Velocity Magnitude (m/s)
126kph

Pathlines Colored by Velocity Magnitude (m/s)
162kph

Figure 7: Pathlines for different values of car speed.

References

[1] R. Baudille, M.E. Biancolini, “Dynamic analysis of a two stroke engine reed valve”, XXXI AIAS Conference, Parma, Italy, (2002).

[2] Battistoni M., Grimaldi C. N., Baudille R, Fiaccavento M. and Marcacci M., "Development of a Model for the Simulation of a Reed Valve Based Secondary Air Injection System for SI Engines", SAE Paper 2005-01-0224 – Proceedings of the 2005 SAE World Congress, April 11-14, 2005, Detroit, USA, edited by SAE International, Warrendale, PA, USA (2005).

[3] R. Baudille, M. E. Biancolini, “FSI Makes FLUENT More Flexible”, Fluent News VOL XIV – Spring 2005 Published by Fluent Inc 10 Cavendish Court Lebanon, NH 03766 USA (2005).

[4] R. Baudille, M. E. Biancolini, “Modelling FSI problems in FLUENT: a dedicated approach by means of UDF programming”, Proceedings of the European Automotive CFD Conference, Frankfurt, Germany (2005).

[5] M. E. Biancolini, R. Baudille, “Modelling FSI Problems in FLUENT: a General Purpose Approach by Means of UDF Programming”, Congresso FISITA 2006 F2006M235 (2006).

[6] Baudille, M. E. Biancolini, “A general approach for studying the motion of a cantilever beam interacting with a 2D fluid flow” Interaction and Multiscale Mechanics, Vol. 1, No. 4 000-000 1 (2008).

[7] Angeletti, M.E. Biancolini, E. Costa, M. Urbinati, “Optimisation of reed valves dynamics by means of Fluid Structure Interaction”, European Automotive Simulation Conference (EASC), 6-7 July 2009, Munich, Germany (2009).

[8] Masud, M. Bhanabhagvanwala, R.A. Khurram, An adaptive mesh rezoning scheme for moving boundary flows and fluid–structure interaction Computers and Fluids Volume: 36, Issue: 1, January, 2007, pp. 77-91 (2007).

[9] F. Bos, Moving and deforming meshes for flapping flight at low Reynolds numbers. Retrieved 28/2/2011 from http://www.openfoamworkshop.org/08/presentations/Mesh/frankBos.pdf (2008)

[10] de Boer, M.S. van der Schoot & H. Bijl, Mesh deformation based on radial basis function interpolation, Computers and Structures Volume: 85, Issue: 11-14, June - July, 2007, pp. 784-795 (2007).

[11] S. Jakobsson, O. Amoignon, Mesh deformation using radial basis functions for gradient based aerodynamic shape optimization, Computers and Fluids Volume: 36, Issue: 6, July, 2007, pp. 1119-1136 (2007).

[12] RBF Morph Web Portal. RBF Web Portal – home page. Retrieved 28/2/2011 from http://www.rbf-morph.com/ (2009).

[13] M.E. Biancolini, C. Biancolini, E. Costa, D. Gattamelata, P.P. Valentini, Industrial Application of the Meshless Morpher RBF Morph to a Motorbike Windshield Optimisation, European Automotive Simulation Conference (EASC) 6-7 July 2009, Munich, Germany (2009).

[14] M.E. Biancolini, Mesh Morphing Accelerates Design Optimization ANSYS Advantage - Volume IV, Issue 1, (2010).

[15] M.E. Biancolini, Mesh morphing and smoothing by means of Radial Basis Functions (RBF): a practical example using Fluent and RBF Morph, Handbook of Research on Computational Science and Engineering: Theory and Practice (in press) (2011).

[16] M.E. Biancolini, U. Cella, “An advanced RBF Morph application: coupled CFD-CSM Aeroelastic Analysis of a Full Aircraft Model and Comparison to Experimental Data”, Proceedings of the 8th MIRA International Vehicle Aerodynamics Conference, 13-14 October 2010, Oxford, UK (2010).

[17] S. Keye, “Fluid-structure coupled analysis of a transport aircraft and comparison to flight data”, 39th AIAA Fluid Dynamics Conference AIAA-2009-4198 (2009).